FIRE BEHAVIOUR OF *CASUARINA EQUISETIFOLIA* PLANTATIONS IN SOUTHERN CHINA AND PREDICTIONS FROM ROTHERMEL MODEL

PAN, D.[1] – PAN, G.[2] – YU, P. Y.[3*]

[1]*Central South Academy of Inventory and Planning of National Forestry and Grassland Administration, Changsha 410014, China*

[2]*College of Life Science and Technology, Central South University of Forestry and Technology, 498 South Shaoshan Road, Changsha, Hunan 410004, China*

[3]*Upgrading Office of Modern College of Humanities and Sciences of Shanxi Normal University, 501 West Binhe Road, Linfen, Shanxi 041000, China*

**Corresponding author*

e-mail: 702487008@qq.com

(Received 27th Jan 2023; accepted 27th Apr 2023)

Abstract. Research on the prediction and prevention of forest fires and the assessment of post-disaster losses has always been a hot topic in the fields of forest ecosystem development and change. In this study, *Casuarina equisetifolia* plantations were selected as the dominant tree species in the typical area of Wanning, Hainan province, southern China. The results revealed that the potential of fire in *C. equisetifolia* plantations were low-and medium-intensity. The surface fire intensity was within 3600 kJ/m^2, the flame length was less than 0.9 m in the absence of wind, the fireline intensity was less than 230 kw/m, and the surface fire spread rate was less than 4 m/min. All *C. equisetifolia* plantation fire types were surface fires, except for the P3 forest type. Overall, this study provides recommendations for forestry managers to adopt appropriate strategies to reduce forest susceptibility to fire and moderate its ecological effects.

Keywords: *canopy fire, forest potential fires, combustible substances, combustible load, Rothermel model*

Introduction

Forest fires are among the strongest perturbation factors in forest ecosystems (García-Llamas et al., 2019; Gonçalves and Sousa, 2017). With the impact of anthropogenic activities and shifts in the global climate, forest fires have intensified over the past 10 years. Devising an effective method to predict forest fire hazards has become a top priority in the field of forest fire research (Rajasekaran et al., 2015). Globally, over 220,000 forest fires occur per year, and more than 6.4 million hm^2 of forests are affected, accounting for more than 0.23% of the forests of the world (Zhu et al., 2019; Zhang et al., 2020).

Forest fires can be devastating and can cause radical changes in the forest ecosystems and permafrost environment leading to human life and infrastructure damage (Li et al., 2021). For example, in 2015, 3,703 forest fires occurred throughout China, including one particularly serious fire, resulting in losses of approximately 400 million yuan in total (Zhu et al., 2019). According to González-De Vega et al. (2016), wildfires are expected to increase in size and severity in the future due to a combination of climate change and land use/land cover (González-De Vega et al., 2016). Frequent forest fires,

http://www.aloki.hu ● ISSN 1589 1623 (Print) ● ISSN 1785 0037 (Online)
DOI: http://dx.doi.org/10.15666/aeer/2104_30753094

especially heavy forest fires, are difficult to suppress (Holden et al., 2009); they damage the natural ecosystem while simultaneously releasing carbon-containing greenhouse gases (Hu et al., 2007), which have caused significant socio-economic damage leading to major ecological consequences (Pausas and Paula, 2012). For example, fire denatures the soil organic matter and changes the input and output processes of soil nutrients and other biogeochemical processes by burning the surface litter layer and the humus layer in the forest at high temperatures (Li et al., 2020a; Bridges et al., 2019); it also alters the water holding capacity of the soil and the formation process of surface runoff that results in soil erosion. Additionally, elevated temperatures change the microflora and species composition of ecological and hydrological conditions in a short period of time (Taş et al., 2014; Zhou et al., 2019), which, in turn, directly or indirectly affect the material circulation and energy flow of forest ecosystems.

Presently, research on forest fires in forest ecosystems is concentrated on a large scale (Verma and Jayakumar, 2018). Most of the existing literature has focused on the physical and chemical properties of forest fires in a specific region of Northeast China (Li et al., 2020a; Zhang et al., 2012). In contrast, the forest region in southern China is characterized by complex landforms, a high degree of forest fragmentation, a small fire area with high fire frequency, and the rescue process is highest in the tropical evergreen broadleaf forest zone due to the influence of topographical factors (Wu et al., 2019). Wanning, located in the tropical region of Hainan, is a large forest province in China and an important source of timber in the south. Due to its unique climate and topographic characteristics, it has become a region with highly frequent forest fires in southern China.

Casuarina equisetifolia plantations play an irreplaceable role in maintaining the balance of the regional ecological system in the tropical region of China, which has high ecological and economic value (Dai et al., 2017; Bai et al., 2021). However, *C. equisetifolia* plantations in southern China are mostly artificial pure forests planted in a large area with a single level and simple structure that increases the potential fire risk (Splawinski et al., 2019).

Therefore, in this study, we aimed to evaluate the relationship between forest fire behavior characteristic parameters and the occurrence of 188, 300.5 ha forest fires in a fire-prone tropical forest ecosystem dominated by *C. equisetifolia* in Wanning, located in the south of China, Hainan Province, for ~ 50 years and to offer their development situations based on five-time forest inventory data. Specifically, our objectives were to: (i) determine the correlation between potential fire risk and forest fire behavior characteristics based on the spatial distribution characteristics and physical traits of combustible beds in *C. equisetifolia* plantations in typical tropical regions, and (ii) evaluate whether Rothermel model can be a valid tool for understanding how pre-fire vegetation structural characteristics control fire severity.

Study site and data collection

Study site

The study site is located in Wanning city in southeast Hainan province (110° 00’ - 110° 34’E, 18° 35’ - 19° 06’N) (*Fig. 1*). The region is characterized by tropical maritime monsoon climate with abundant sunshine, concentrated rainfall, and high temperatures. The annual average temperature is 23.0°C, the coldest average temperature is 18.7°C in January. The hottest temperature is 28.5°C in July, the

http://www.aloki.hu ● ISSN 1589 1623 (Print) ● ISSN 1785 0037 (Online)
DOI: http://dx.doi.org/10.15666/aeer/2104_30753094

average annual rainfall in coastal areas is 2100–2200 mm, the annual average sunshine is 1500–2200 h, accounting for 36%–50% of the available hours, and the main soil type was lateritic (Huan-Ting et al., 1994; Geng et al., 2022; Ji et al., 2022). Natural disasters in Wanning include wind, drought, floods, insects, and lightning. Among these, drought attacks caused by elevated temperatures and little rain are the main natural disasters in this city. The forest in this region is dry and flammable, so it can easily cause forest fires, which often cause varying degrees of loss to crops, people's lives, and properties.

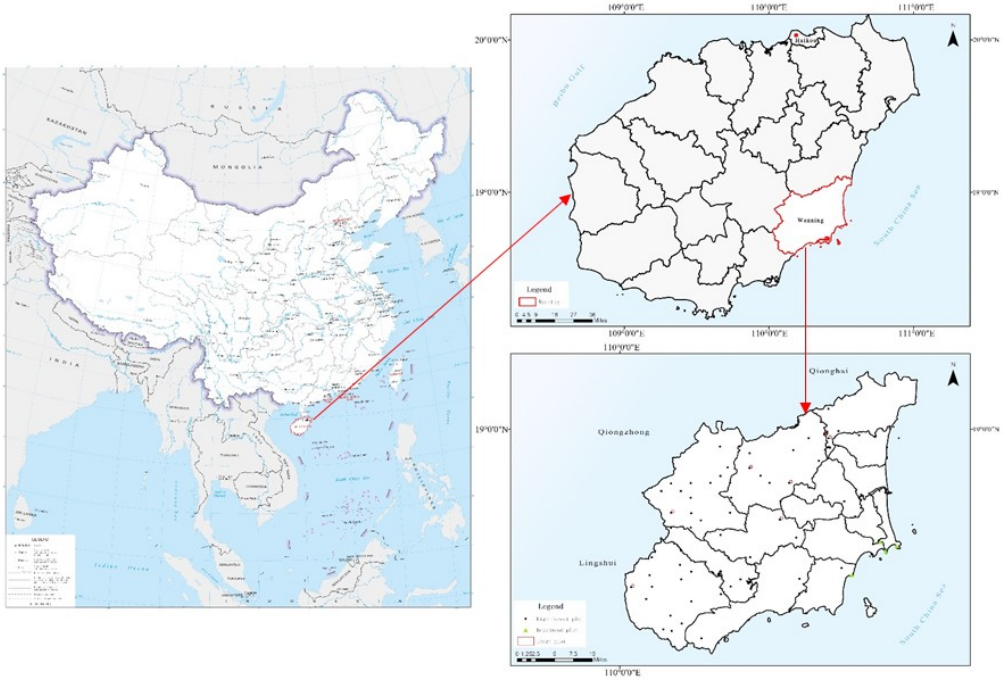

Figure 1. *Location map of the study area (Wanning, Hainan province)*

The sample set

C. equisetifolia plantations of five different ages with similar site conditions were selected from the forest from May–June, 2013. Five plots with ages of 10, 18, 20, 30, and 50 years were set and named as P1, P2, P3, P4, and P5, respectively. All the selected stands were *C. equisetifolia* plantations without human disturbance and with no fire records over 30 years. Simultaneously, five 2 m × 2 m shrub quadrats, five 2 m × 2 m fallen woody quadrats, five 1 m × 1 m non-woody (herbaceous and fern) quadrats, five 1 m × 1 m litters quadrats, and five 0.5 m × 0.5 m humus quadrats were set in each 400 m^2 plot by the diagonal method. The coordinates of the sample plot, including the stand characteristics of altitude (M), slope (°), slope aspect, canopy density, species name, diameter at breast height (DBH, cm), tree height (H, M) were recorded (*Table 1*).

Survey of combustible bed

The trees and shrubs in the forest were divided according to the Chinese forestry industry standard LY/T 1952–2011, for each tree (DBH > 1 cm), crown base height and branch height were recorded for shrubs (DBH ≤ 1 cm), and height, coverage, and crown

http://www.aloki.hu ● ISSN 1589 1623 (Print) ● ISSN 1785 0037 (Online)
DOI: http://dx.doi.org/10.15666/aeer/2104_30753094

width were recorded. A 2 m × 2 m sample was cut using the total harvest method, and the aboveground part of the shrub in the square was weighed and then brought back to the laboratory to calculate the water content. The aboveground parts of all herbs, vines, ferns, and other ground cover plants in the 1 m × 1 m plots were harvested. The same method was used to measure moisture content and calculate non-wood fuel load per unit area proportionally. All the litter in the 1 m × 1 m plots, primarily undecomposed branches, grass, vines, leaves, and cones were harvested. The average thickness of litter in the quadrat was me-asured along the S-shaped route, and its flat mean was taken, and the coverage of litter in the quadrat was estimated.

Table 1. *Fuelbed characteristics of different ages C. equisetifolia plantation*

Index	P1[§]	P2	P3	P4	P5
1 h fuel load (t/hm^2)	5.10	5.18	5.39	7.25	6.83
10 h fuel load (t/hm^2)	2.42	2.84	2.95	3.64	3.11
100 h fuel load (t/hm^2)	0.3	0.3	0.5	0.7	0.4
Fresh herbage fuel load (t/hm^2)	0.06	0.09	0.12	0.15	0.14
Thickness of combustible bed (m)	0.20	0.22	0.26	0.25	0.25
Dead combustible heat (kJ/kg)	19026	19026	19026	19026	19026
Live combustible heat (kJ/kg)	19026	19026	19026	19026	19026
Canopy height (m)	13.0	15.5	16.5	17.0	18.5
Comb base height (m)	3.4	3.5	4.7	3.8	3.7
Canopy volumetric weight (kg/m^3)	0.37	0.39	0.41	0.36	0.34
Wind speed adjusted factor	0.19	0.19	0.28	0.28	0.23
Combustible concealment (%)	75	85	90	90	90
Gradient	30	35	35	40	40

[§]P1, P2, P3, P4 and P5 refer to *C. equisetifolia* plantations of five different ages with 10, 18, 20, 30, and 50 years, respectively, the same as below

Determination of combustible ash

The ash content of straw, irrigation, grass, and litter samples collected from the standard plot was determined according to the Chinese forestry industry standard LYT 1268–1999. The determination steps were as follows: (1) The samples were collected and kept in the baking oven (TX—SX0, SuZhou Tai De Oven Equipment Manufacturing Co., Ltd., Suzhou, China), then toasted at 105℃ for 30 min, and then adjusted to 80℃; toasted until a constant weight was achieved. (2) The dried samples were powdered using the powder prototype (LD-2000, CHANGSHA HONGJING MECHANICAL EQUIPMENT CO., LTD., Changsha, China); 10 g of each sample was kept in the cleaned porcelain crucible; they were then numbered, weighed, and step one was repeated. (3) The porcelain crucible (szkftt2022121910, Kaifate Pottery Co., LTD., Suzhou, China) was kept in the universal furnace (WY88-FL-1, Dongfang glass Co., LTD., Beijing, China) to heat the sample, slowly make it smoke, and carbonize it until smoke was no longer produced, and then the heat was turned off. (4) The porcelain crucible was kept in the muffle furnace (KF1200-VI-I, Tianjin Maafur Technology Co., LTD., Tianjin, China) with the temperature set at 600℃ for 8 h, after which the sample was removed, powdered to ash, and kept in a dryer; it was then cooled down to constant weight and weighed. The formula used for calculating combustible ash was:

http://www.aloki.hu ● ISSN 1589 1623 (Print) ● ISSN 1785 0037 (Online)
DOI: http://dx.doi.org/10.15666/aeer/2104_30753094

$$S = \frac{W_A - W_C}{W_B - W_C} \quad \text{(Eq.1)}$$

where S is the fuel ash content (%), W_A is the total weight after ashing (g), W_B is the total weight before carbonization, and W_C is the weight of the porcelain crucible (g).

Calculating the calorific value of fuel

The calorific value of combustion was used to calculate forest fire intensity and spread speed. A PARR 6300 oxygen bomb calorimeter (PARR 6300, Parr Instrument Company, NV, USA) was used to analyze the samples. The determination steps are as follows: (1) The sample was oven-dried to a constant weight, and then ground to a powder. (2) One gram of each powdered sample was pressed into a 1 g powder cake. (3) The powder was placed into a fine and clean porcelain crucible, dried again to a constant weight, and weighed. (4) The porcelain crucible loaded with samples was placed into the calorimeter; at this time, the oxygen bomb was automatically filled with oxygen, and the initial heat balance was established. (5) Finally, the calorimeter automatically adopted the constant temperature mode for measurement, recorded the heat exchange capacity in the bucket, modified the measurement results, and provided the results. According to the calorific value of the different components of combustible materials and the proportion of the whole plant, the average calorific value of the whole tree species can be obtained from the weighted average calorific value.

Calculation of reaction intensity of fuel combustion

The reaction intensity of each fuel unit can be calculated using the following formula by weighting the load of each species:

$$I_R = \tau \sum_{i=1}^{n} F_{ij} W_{nij} H_i \mu_{si} \mu_{Mi} \quad \text{(Eq.2)}$$

Among them:

$$W_m = \sum_{i=1}^{n} F_{ij} W_{nij} = \sum_{j=1}^{n} \frac{F_{ij} W_{oij}}{1+S_{ij}} \quad \text{(Eq.3)}$$

$$H_i = \sum_{i=1}^{n} F_{ij} H_{ij} \quad \text{(Eq.4)}$$

$$\mu_{si} = 0.174 S_{ei}^{-0.19} \quad \text{(Eq.5)}$$

$$S_{ei} = \sum_{j=1}^{n} F_{ij} S_{eij} \quad \text{(Eq.6)}$$

$$\mu_{Mi} = 1 - 2.59\left(\frac{M_{fi}}{M_{Xi}}\right) + 5.11\left(\frac{M_{fi}}{M_{Xi}}\right)^2 - 3.52\left(\frac{M_{fi}}{M_{Xi}}\right)^2 \quad \text{(Eq.7)}$$

$$M_{fi} = \sum_{j=1}^{m} F_{ij} M_{fij} \quad \text{(Eq.8)}$$

$$\tau = \tau_{max}\left(\frac{\beta}{\beta_{op}}\right)^A exp\left[A\left(1 - \frac{\beta}{\beta_{op}}\right)\right] \quad \text{(Eq.9)}$$

http://www.aloki.hu ● ISSN 1589 1623 (Print) ● ISSN 1785 0037 (Online)
DOI: http://dx.doi.org/10.15666/aeer/2104_30753094

$$\tau_{max} = \frac{\sigma^{1.5}}{495+0.0594\sigma^{1.5}} \quad \text{(Eq.10)}$$

$$\sigma = \sum_{i=1}^{n} F_{ij}\sigma_i = \sum_{i=1}^{n}\sum_{j=1}^{m} F_{ij}\sigma_{ij} \quad \text{(Eq.11)}$$

$$\beta = \frac{1}{\delta}\sum_{i=1}^{n}\sum_{j=1}^{m}\frac{W_{ij}}{\rho_{pi}} \quad \text{(Eq.12)}$$

$$\rho_b = \frac{1}{\delta}\sum_{i=1}^{n}\sum_{j=1}^{m} W_{ij} \quad \text{(Eq.13)}$$

where I_R is the reaction intensity of fuel, Btu/(ft^2·min); τ is the potential reaction rate, 1/min; W_{ni} is class I fuel net load, lb/ft^2; W_{oij} is the combustible load quantity of class i grade j, lb/ft^2; S_{ij} is the combustible mineral content of class i grade j; W_{nij} is combustible net load of class i grade j, lb/ft^2; H_i is the average calorific value of in class i, Btu/lb; H_{ij} is the average calorific value of class i grade j, Btu/lb; μ_{si} is he fuel mineral inhibition coefficient of class i; S_{ei} is the combustible effective ore quality factor of class i; S_{eij} is the effective mineral system of combustible of class i grade j; μ_{Mi} is the combustible water retardation factor of class i; μ_{Mij} is the fuel water block coefficient of class i grade j; M_{xj} is the combustible-quenched moisture content of grade j; τ_{Max} is maximum reaction rate, 1/min; σ is the surface volume ratio of fuel, 1/ft; σ_{ij} is the combustible surface volume ratio of class i grade j, 1/ft; β is the average compactness; β_{op} is the optimal compactness; ρ_b is the average volume density, lb/ft^3; δ is fuel thickness, ft; ρ_{pij} is the basic density of combustible of class i and class j, lb/ft^3.

Calculation of forest fire spreading speed

The calculation of the forest fire spreading speed is based on Byram (1959), and the relevant formula is:

$$R = \frac{IR\zeta(1+\Phi_W+\Phi_s)}{\beta_b \varepsilon Q_{ig}} \quad \text{(Eq.14)}$$

Among them:

$$\zeta = (192 - 0.259\sigma)^{-1} exp[(0.792 + 0.681\sigma^{0.5})(\beta + 0.1)] \quad \text{(Eq.15)}$$

$$\varepsilon Q_{ig} = \sum_{i=1}^{n} F_i \sum_{j=1}^{m} F_{ij} exp\left(\frac{-138}{\sigma_{ij}}\right) Q_{igij} \quad \text{(Eq.16)}$$

$$Q_{igij} = 250 + 1116M_{fij} \quad \text{(Eq.17)}$$

$$\Phi_W = CUB\left(\frac{\beta}{\beta_{OP}}\right)^{-E} \quad \text{(Eq.18)}$$

$$\Phi_S = 5.275\beta^{-0.3}(\tan\theta)^2 \quad \text{(Eq.19)}$$

$$C = 7.47exp(-0.133\sigma^{0.55}) \quad \text{(Eq.20)}$$

$$B = 0.02526\sigma^{0.54} \quad \text{(Eq.21)}$$

http://www.aloki.hu ● ISSN 1589 1623 (Print) ● ISSN 1785 0037 (Online)
DOI: http://dx.doi.org/10.15666/aeer/2104_30753094

$$E = 0.715exp(-3.59 \times 10^{-4}\sigma) \quad \text{(Eq.22)}$$

where R is the forest fire spreading speed, ft/min; I_R is the forest fire reaction intensity, Btu/(ft^2·min); ζ is the ratio of calm flux; ΦW and ΦS are wind and slope influence coefficients, respectively; ρ_b is the fuel density, lb/ft^3; ε is the heating coefficient related to density; Qig is the ignition unit of heat required for combustibles by weight, Btu/lb; U is applied to the flame wind speed, ft/min; θ is slope, °; *and* C, B, and E are correction coefficients.

Calculation of forest fire behavior

(1) Forest fire intensity

Forest fire intensity refers to the energy released by forest fires within a unit length of the fireline per unit time, also known as fireline intensity. The formula for calculating the forest fire intensity can be derived according to the classical formula proposed by Byram (1959).

$$I = \frac{H \times W \times R}{600} \quad \text{(Eq.23)}$$

where I is the forest fire intensity (Kw/m), H is the calorific value of fuel (J/g), W is the effective fuel load (t/hm^2), R is the spreading speed of the forest fire (m/min), and 1/600 is the conversion coefficient from British to metric units.

(2) Flame length

Flame length refers to the length of the continuous flame after ignition of the combustible bed; therefore, a flying fire was not included. The formula for calculating the forest fire intensity can be derived according to the formula proposed by Byram (1959).

$$L = 0.077\,476 I^{0.46} \quad \text{(Eq.24)}$$

where L is the flame length (m), I is the forest fire intensity (kw/m), and 0.077476 is the conversion coefficient.

(3) Flame height

In the absence of wind, the flame form is vertical and upward, and the flame length is the flame height. In the case of wind, the spread speed of the flame is affected, and the flame tilts under the influence of wind speed. Currently, the height is less than the length, and the height calculation formula is as follows:

$$h = L_w = 0.77476 I^{0.46} = 0.077476 \left(\frac{H \times W \times R_w}{600}\right)^{0.46} \quad \text{(Eq.25)}$$

where h is the flame height (m), L_w is the forest fire affected by wind speed (Kw/m), *and* R_w is the spread speed of forest fire under the influence of wind speed (m/min). When the wind speed is 0 m/s, Rw = R.

http://www.aloki.hu ● ISSN 1589 1623 (Print) ● ISSN 1785 0037 (Online)
DOI: http://dx.doi.org/10.15666/aeer/2104_30753094

Spot firing test

Test materials were obtained from the litter layer for each age stand. The design method used was the incomplete block test with three repetitions, because the ignited combustible bed components were from the standard sample plot, and the Rothermel model is insensitive to the thickness of the combustible bed (Andrews et al., 2013; Rothermel, 1972). Therefore, in this study, the water content and load were taken as control variables, while the mixing proportion of combustible bed components and layer thickness were set as constants (*Fig. 2*). Water content was set at three levels: 10%, 15%, and 20%, and the load capacity was set at three levels: 4 t/hm^2, 5 t/hm^2, and 6 t/hm^2. The mixing ratio was the natural mixing ratio of each standard plot, and the thickness of the combustible bed was 4 cm, A total of 135 spot-firing tests were conducted.

The spot-burning test bed was 2 m long and 1 m wide, and a 1 m high pole was placed every 10 cm to fix the thermocouples (WRN-130, Jiangsu Unison Industrial Measurement Control System Co., LTD., Jiangsu, China). It was used to measure the temperature of the combustible bed in the burning process, and the burning speed was measured with a stopwatch. The moisture content of the combustible was determined using an oven and a rapid moisture-measuring instrument. A 2-m long fire source zone (linear fire zone with ethanol) was set at the front end of the ignition bed so that the flame was close to the steady state when it reached the combustible bed, and the ash was collected after complete combustion to measure the amount of combustible consumption (*Fig. 2*). The random error of the thickness of the combustible bed was controlled within ±0.5 cm, the change in ambient temperature was controlled within ±2°C by air conditioning, and the change in air relative humidity was controlled within ± 15%.

Figure 2. *The test of spot firing*

Data processing

The calculation of potential fire behavior characteristics of *C. equisetifolia* plantations is based on the classical formula proposed by Rothermel (1972) and Byram (1959). A load-weighted simulation was completed with the combined

http://www.aloki.hu ● ISSN 1589 1623 (Print) ● ISSN 1785 0037 (Online)
DOI: http://dx.doi.org/10.15666/aeer/2104_30753094

measured data from the sample site and the analysis results of the indoor fuel characteristics. the simulation results were considered acceptable if the average relative error was < 30%. The simulation results for the forest fire spreading speed, reaction intensity, and flame height were compared. The formula for calculating the average relative error is

$$MRE = \frac{\left(\sum_{i=1}^{n}\left|\frac{y_i - y_j}{y_i}\right|\right)}{n} \quad \text{(Eq.26)}$$

where MRE is the average relative error; y_i is the observed value of the point burning test; y_j is the simulated value of the eigenvalue weighted by the load; n is the point firing test.

Results

Proof of simulated result

The scattered points of the simulated and observed values of each stand were evenly distributed on both sides of the line y = x, indicating that the spread rate calculated after weighting had a good effect (*Fig. 3*). The mean relative errors of each stand were 8.22% (P1), 8.61% (P2), 13.98% (P3), 25.77% (P4), and 26.04% (P5). The fitting effect of the P1 was the best, while the fitting effect of the P4 was the worst. Additionally, it was observed that, in the same forest when the spread rate gradually increases, the fitting degree will be lower.

The average relative errors of each stand were 24.71% (P1), 25.02% (P2), 25.03% (P3), 28.15% (P4) and 24.53% (P5), respectively (*Fig. 4*). The fitting effect was the best for P5 and the worst for P4. The fitting of the firewire intensity also tended to increase with an increase in deviation. With the acceleration of the spread rate of the firewire and the increase in the flame height, the intensity of the firewire also increases, which is in linear.

The scattered points of P5 have all moved below the straight line, and with the increase in stand age, the surface 1 h and 10 h combustibles increase (*Fig. 5*). These two types of combustibles are small combustibles, and their contribution to flame height is greater than that of 100 h combustibles. However, the load weight is less important than that of the 100 h combustibles, resulting in the simulation results being lower than the actual observation results. The average relative errors of each stand were 7.41% (P1), 8.72% (P2), 15.01% (P3), 25.73% (P4), and 24.97% (P5). The fitting effect of the P1 was the best, while the fitting effect of the P5 stand was the worst.

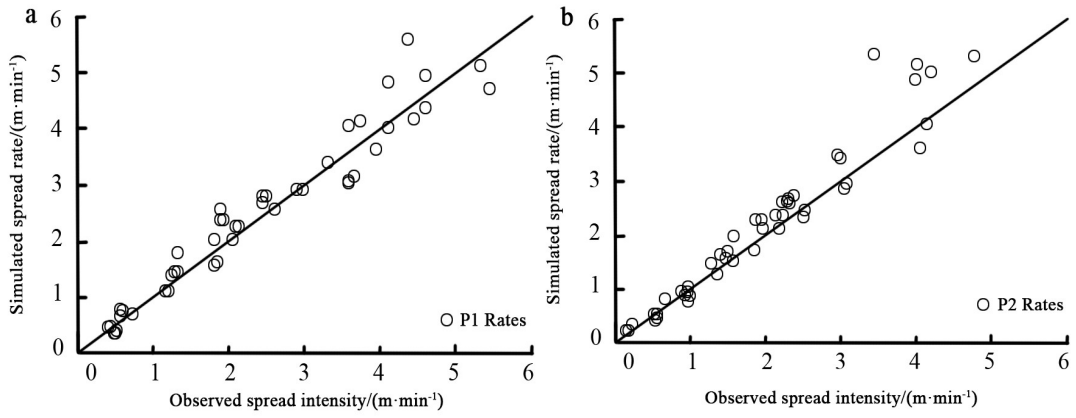

http://www.aloki.hu ● ISSN 1589 1623 (Print) ● ISSN 1785 0037 (Online)
DOI: http://dx.doi.org/10.15666/aeer/2104_30753094

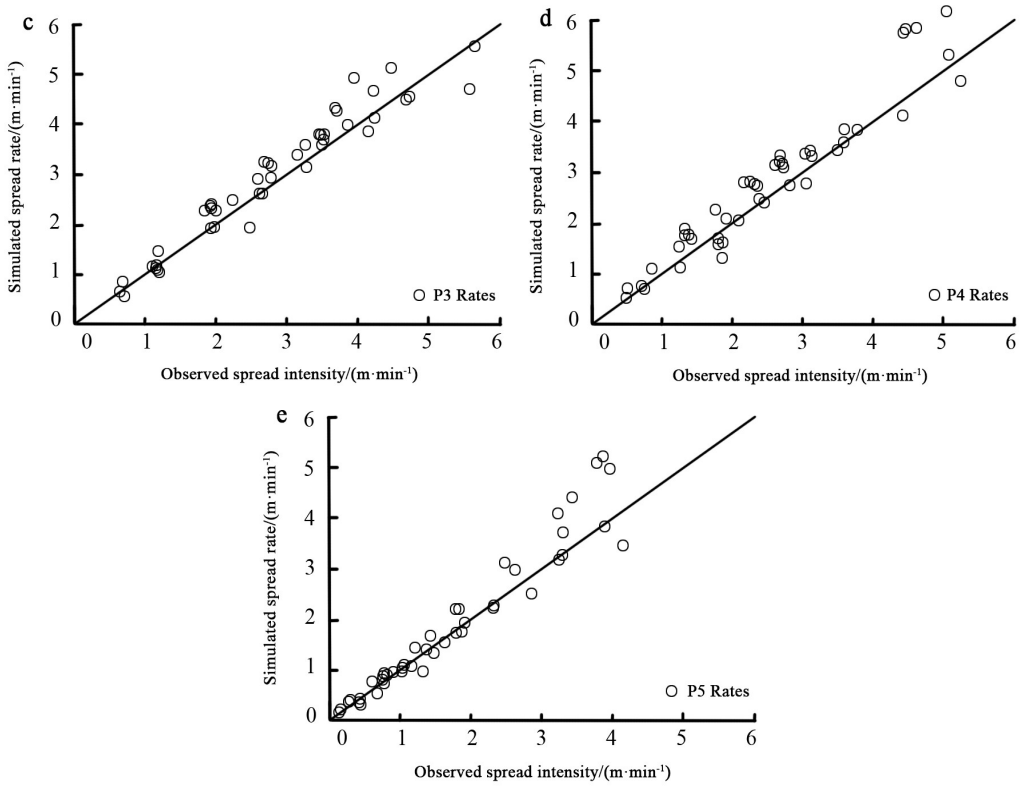

Figure 3. *Comparison of predicted and observed rate of simulated (ROS) values in different forests*

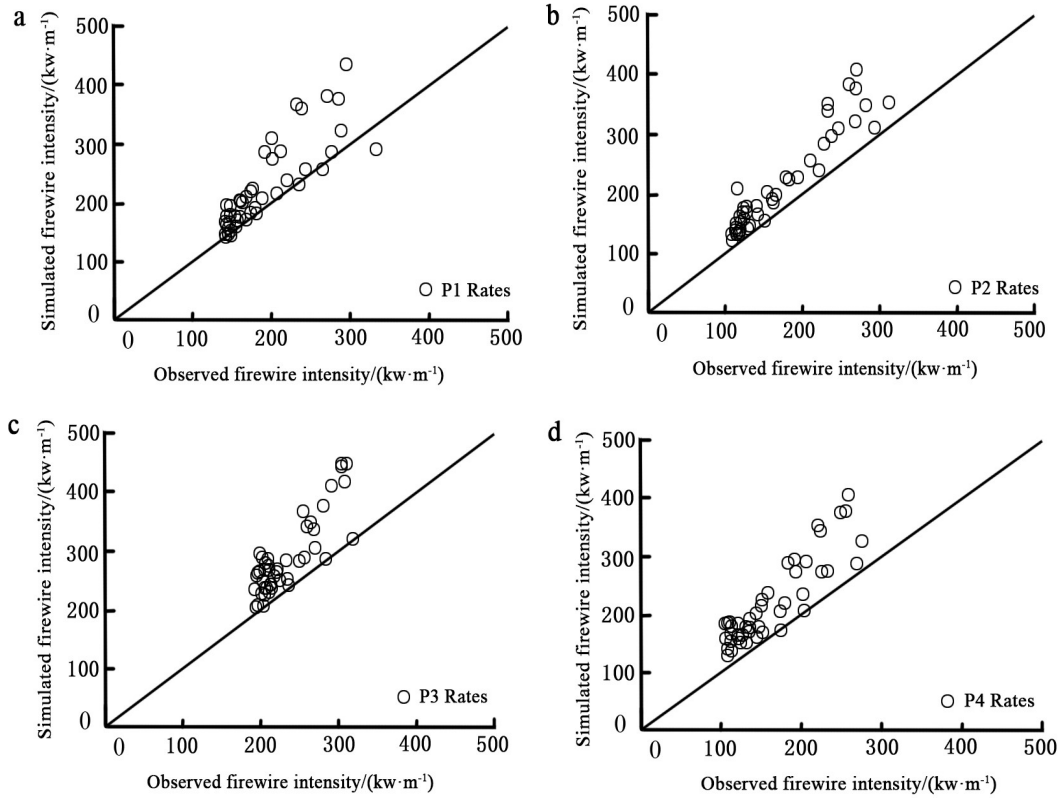

http://www.aloki.hu ● ISSN 1589 1623 (Print) ● ISSN 1785 0037 (Online)
DOI: http://dx.doi.org/10.15666/aeer/2104_30753094

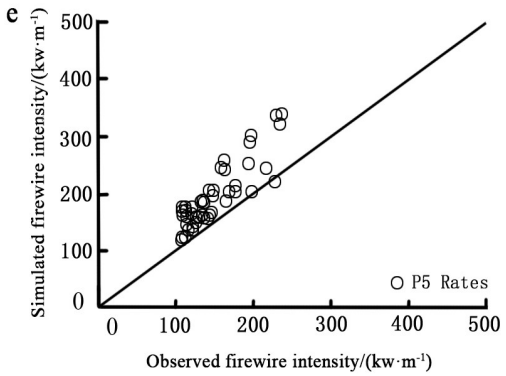

Figure 4. *Comparison of surface fire behavior of C. equisetifolia plantations at different ages*

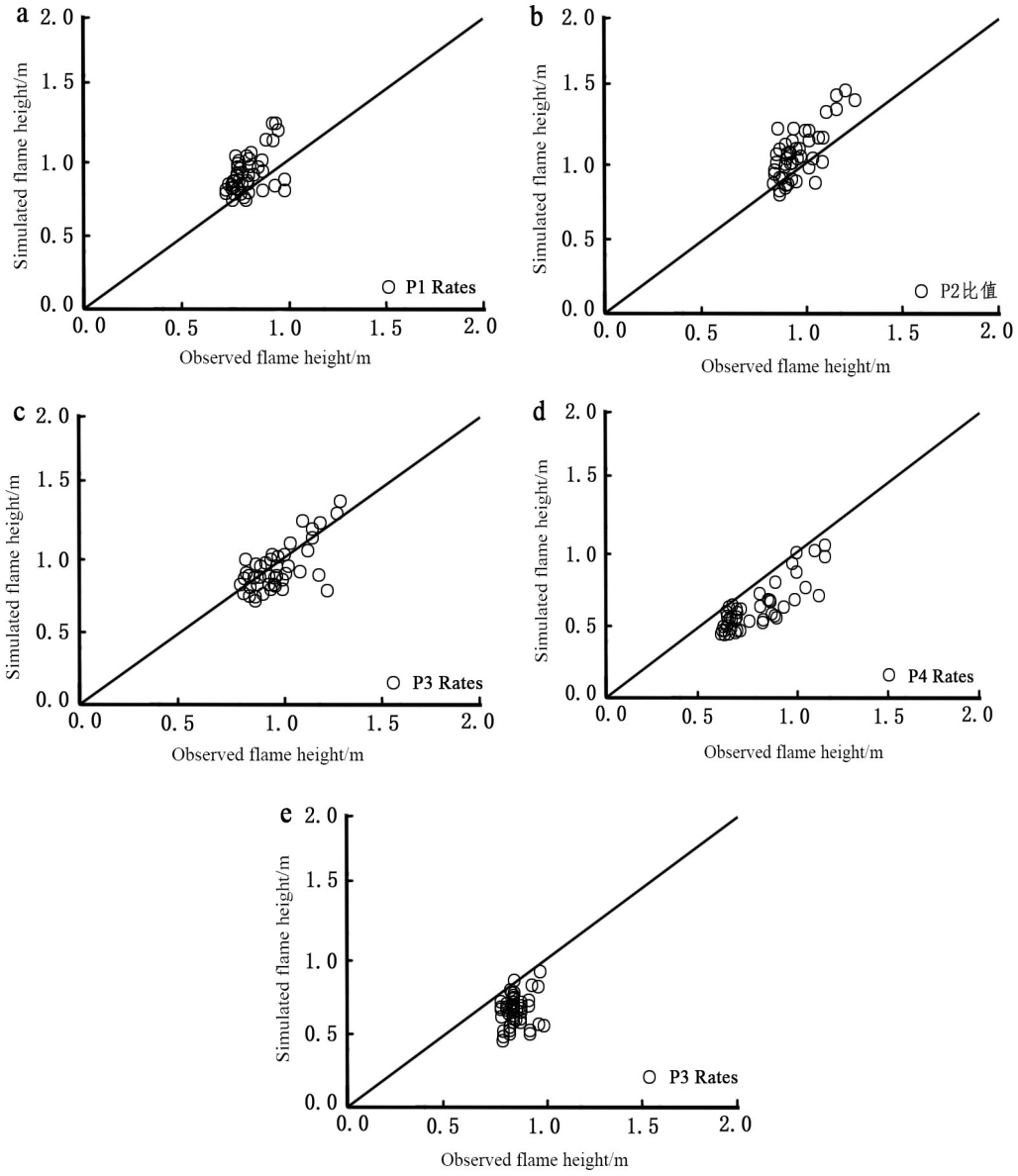

Figure 5. *Comparison of predicted and observed values of fire length in different forests*

http://www.aloki.hu ● ISSN 1589 1623 (Print) ● ISSN 1785 0037 (Online)
DOI: http://dx.doi.org/10.15666/aeer/2104_30753094

Comparison of surface fire behavior of combustible models of C. equisetifolia plantations at different ages

The variation trends of the surface fire spreading velocity, fireline intensity, and flame length of *the C. equisetifolia* plantations at various ages and wind speeds were shown (*Fig. 6*). The results showed that the surface fire behavior of *C. equisetifolia* plantations at different forest ages increased with increasing wind speed. The order of the parameter values of the three indicators was essentially the same (P3 > P1 > P4 > P2 > P5). This means that the fire behavior of the *C. equisetifolia* plantation (P3) was higher than that of the other stands, and lowest at P5, but still showed a trend of linear increase with the increase in wind speed (*Fig. 6*). The surface fire spread velocity reached 0.9 m/min and the fireline intensity reached 227 kw/m when there was no wind. When the wind speed increased to 5 m/s, the surface fire spreading speed of the P3 forest type increased to 1.6 m/min and the fireline intensity increased to 229 kW/m. When the wind speed increased to 30 m/s, the surface fire spreading speed of the P3 forest type was 5.9 m/min and the fireline intensity was 367 kw/m, which was 1.90 times and 1.85 times that of P5, respectively (*Fig. 6a*). The surface flame length of each forest type increased with increasing wind speed, but the increase was not significant, and the flame length changed a little when the wind speed was 0–5 m/s (*Fig. 6c*).

Comparison of canopy fire behavior of combustible models in C. equisetifolia plantations at different ages

The crown fire conversion rate of *C. equisetifolia* plantations at all ages increased linearly with increasing wind speed (*Fig. 7*). The canopy fire conversion rates of P1 and P2 stands reached more than 1 when there was no wind, and the canopy fire conversion rates of P4 and P5 increased with an increase in wind speed, but the maximum was 0.8. When the wind speed was greater than 20 m/s in P2, the conversion rate was greater than 1 (*Fig. 7a*). With the increase in wind speed, the incidence of active crown fire in P3 stand increased significantly, while in other stands, the increase rate was the same, which increased to 1 at approximately 10 m/s (*Fig. 7b*). The spreading speed and flame length were positively correlated with wind speed, and the index of stand of P3 increased the most with the increase in wind speed, while it was lowest in P5 stands (*Fig. 7c, d*). In addition, *C. equisetifolia* plantations in P3 usually have a high density and considerable number of trees per unit area, resulting in a rapid increase in canopy fire intensity with wind speed.

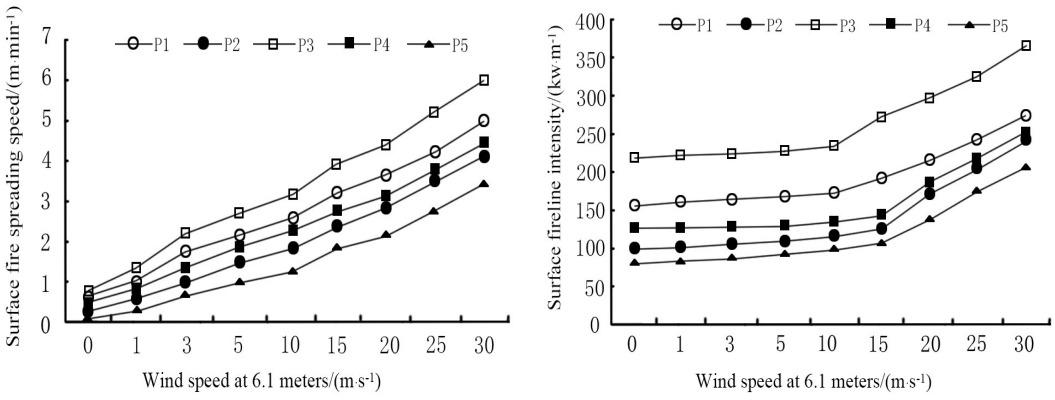

http://www.aloki.hu ● ISSN 1589 1623 (Print) ● ISSN 1785 0037 (Online)
DOI: http://dx.doi.org/10.15666/aeer/2104_30753094

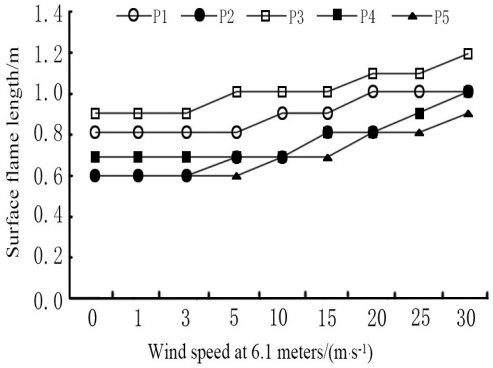

Figure 6. *Comparison of surface fire behavior of combustible models of C. equisetifolia plantations at different ages*

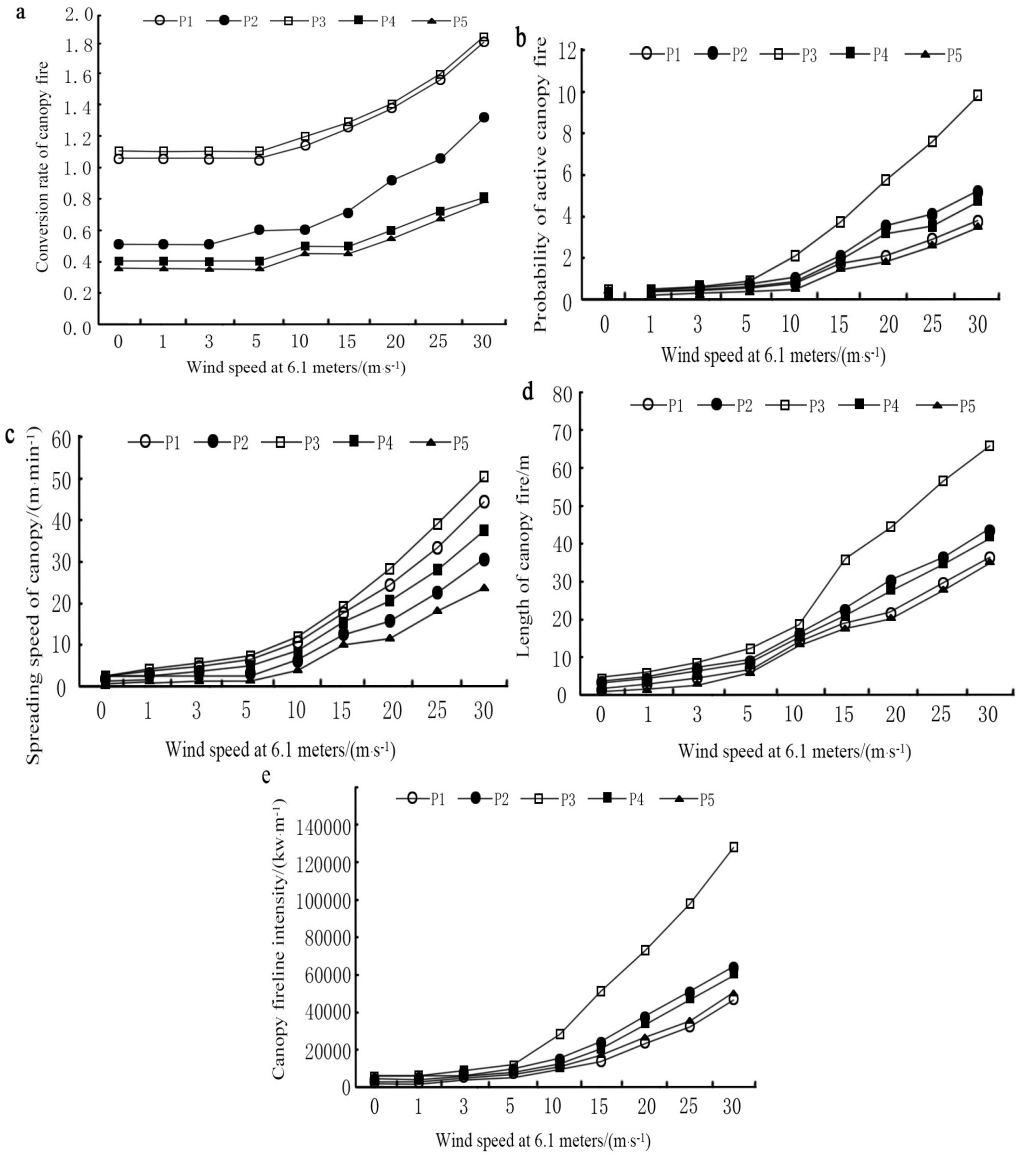

Figure 7. *Comparison of canopy fire behavior of combustible models in C. equisetifolia plantations at different ages*

http://www.aloki.hu ● ISSN 1589 1623 (Print) ● ISSN 1785 0037 (Online)
DOI: http://dx.doi.org/10.15666/aeer/2104_30753094

Fire behavior and types of fuel models in C. equisetifolia plantations

The fire surface intensity of the combustible beds in each stand varied in the range of 3,455–3,599 kJ/m^2 (*Table 2*). There was no significant difference among stands, and the threshold of surface fire intensity in P4 and P5 stands was higher, whereas there was a high probability of crown fires igniting and spreading in P3 stands.

Table 2. *C. equisetifolia plantation potential fire behavior and fire types of the fuel models*

Forest stand		P1	P2	P3	P4	P5
The intensity of fire surface		3590	3698	3699	3640	3550
The intensity threshold of surface fire		180	201	227	311	301
The spread threshold of canopy fire		7.1	6.5	6.2	6.8	6.9
Igniting possibility		13	15	18	21	19
Fire types under different wind speeds	0	Surface-fire	Surface-fire	Intermittent canopy fire	Surface-fire	Surface-fire
	1	Surface-fire	Surface-fire	Intermittent canopy fire	Surface-fire	Surface-fire
	3	Surface-fire	Surface-fire	Intermittent canopy fire	Surface-fire	Surface-fire
	5	Surface-fire	Surface-fire	Smoldering canopy fire	Conditional canopy fire	Surface-fire
	10	Surface-fire	Surface-fire	Smoldering canopy fire	Conditional canopy fire	Conditional canopy fire
	15	Surface-fire	Conditional canopy fire	Smoldering canopy fire	Conditional canopy fire	Conditional canopy fire
	20	Conditional canopy fire	Conditional canopy fire	Smoldering canopy fire	Conditional canopy fire	Conditional canopy fire
	25	Conditional canopy fire	Smoldering canopy fire	Smoldering canopy fire	Conditional canopy fire	Conditional canopy fire
	30	Smoldering canopy fire	Smoldering canopy fire	Smoldering canopy fire	Conditional canopy fire	Conditional canopy fire

Discussion

Comparison of simulated and observed values of forest fire behavior in C. equisetifolia plantations

Forest combustibles are the primary cause of forest fires and form the main body of forest fire behavior; therefore, their combustible characteristics have a significant impact on fire behavior indicators (Kuznetsov et al., 2022; Li et al., 2020b; Wu et al., 2022). These characteristics of fire behavior, such as the spread speed of fire, fire intensity, flame length, and other indicators, play an important role in forest-fire prediction and firefighting methods (Rodrigues et al., 2021; Molina et al., 2022). In this study, the simulated values and observations of forest fire spread rate, forest fire line intensity, and forest fire flame height were compared with the observational values of *C. equisetifolia* plantations of different ages. Based on the generalized Rothermel model (Rothermel, 1972), the simulation results weighted by the combustible loads were compared with the ignition test observations. The fitting pair for the spread rate of forest fire was the best, the simulation value for the intensity of the fire line was high, and the simulation value for the flame height gradually decreased with increasing forest age.

The simulation of the Rothermel model can easily have a certain impact on the spread speed and intensity of forest fires (Andrews et al., 2013; Andrews, 2018). This is because, in the Rothermel model, the combustible bed is set to a porous continuous

http://www.aloki.hu ● ISSN 1589 1623 (Print) ● ISSN 1785 0037 (Online)
DOI: http://dx.doi.org/10.15666/aeer/2104_30753094

homogenization type (Andrews et al., 2013). With the acceleration of the spread rate of the fire line and the increase in the flame height, the strength of the fire line also increases, which is almost linear; in the ignition test, the combustible bed is not completely homogeneous (Porterie et al., 2000), the continuity is lower than the ideal state, and the growth rate of the fireline strength will be slightly lower (Davies and Legg, 2011). However, all results were within acceptable limits and could be used to calculate the potential forest fire behavior characteristics of *C. equisetifolia* plantations in the tropical coastal city of Wanning, Hainan.

Comparison of surface fire behavior of C. equisetifolia plantations at different forest ages

The surface fire behavior of *C. equisetifolia* plantations of different forest ages, including the surface fire spread speed, fire line intensity, and surface flame length, increased linearly with the increase in wind speed, and the fire behavior parameters in the *C. equisetifolia* plantations of 20a (P3) were higher than those of other stands, while they showed the lowest value in the *C. equisetifolia* plantations of 50a (P5) (*Fig. 6*). The thickness of the higher-surface-combustible bed is an important reason for the faster surface fire burning in the *C. equisetifolia* plantations of 20a (Kreye et al., 2020). Page and Jenkins also demonstrated that the thickness and moisture content of the combustible bed are important factors in determining fire behavior (Page and Jenkins, 2007). During the dry season, months of high-temperature and rainless weather will minimize the moisture content of combustibles on the surface, and the probability of ignition is the greatest (McAllister et al., 2012). All fire behavior parameters of the *C. equisetifolia* plantation (P5) over 50 years were the lowest (*Fig. 6*). At low wind speeds, the surface fire spread rate and fireline intensity gain were not significant because the surface combustible bed still contained a certain amount of moisture when it was not ignited, resulting in a pre-combustion process (Kreye et al., 2013). However, when the wind speed is high, the flame is elongated by the wind speed, and the combustible beds are burned by flames before they are ignited. Simultaneously, excessively high temperatures can rapidly reduce the moisture content of the combustible bed, and once ignited, it can quickly enter the flaming combustion stage (Porterie et al., 2000; Wang et al., 2016; Valdivieso and Rivera, 2014; Manzello et al., 2020). Therefore, it is necessary to systematically remove combustible materials from the surface and set a safe crown base height for *C. equisetifolia* plantations of different forest ages (Ascoli et al., 2018; Lands and Fernie, 2022), periodically prune the branches of *C. equisetifolia* plantations, and artificially clear the partition in the vertical distribution direction of combustibles (Khan et al., 2022; Rowell et al., 2016), which can effectively reduce the probability of canopy fire.

Comparison of canopy fire behavior in combustible material models of C. equisetifolia plantations at different forest ages

The canopy fire conversion rate, spread rate, and flame length of the canopy fire of the *C. equisetifolia* plantations at various forest ages were positively correlated with wind speed (McCaw et al., 2012). Our results showed that canopy fire behavior increased linearly with increasing wind speed (*Fig. 7*). Due to the rapid spread rate and large flame length in the 20a *C. equisetifolia* plantations (P3), the high density and larger number of plants per unit area in the P3 plantation resulted in the canopy fire

http://www.aloki.hu ● ISSN 1589 1623 (Print) ● ISSN 1785 0037 (Online)
DOI: http://dx.doi.org/10.15666/aeer/2104_30753094

behavior in P3 being the most severe plantation, which caused severe damage to a large area of forest stands and posed a serious threat to the personal safety of firefighters. Thus, during the windy season, targeted thinning of 20-year-old *C. equisetifolia* plantations is a very effective way to stop forest fires (Crecente-Campo et al., 2009; Molina et al., 2012). In contrast, the canopy fire spread rate and flame length were lowest in P5 plantations (*Fig. 7c, d*), as the aging *C. equisetifolia* plantations in Wanning have not been managed for over 50 years after the traditional rotation age, exacerbating a reduction in crown volume with tree aging (Alteyrac et al., 2006), ultimately resulting in discontinuous flame transmission pathways. However, owing to the abundant oil and fat in the trunk and coniferous leaves of aging stands (Salem et al., 2021), the intensity of the fire hazard generated when burning was not the lowest (*Fig. 7e*). Thus, the transmission route of canopy fires should be cut off when managing forest fires (Roberts et al., 2018).

Fire intensity is an important indicator of the burning intensity of forest canopy fires (Dymov et al., 2021; Petersson et al., 2020). The quantitative assessment of fire intensity, combined with the changes in soil properties and stand structure of *C. equisetifolia* plantations after the fire, could predict the contribution and influence mechanism of different fire intensities on *C. equisetifolia* plantations (Malvar et al., 2013). Our results showed that the combustible beds of fire intensity in P4 and P5 forest stands were much higher after ignition (*Table 2*). According to previous survey of the forest stand, the shrubs in these two forest types were fewer than in other forest stands, which directly resulted in the discontinuity of the distribution of combustibles in the vertical direction (Sullivan et al., 2012), and once the surface combustibles were ignited, the upward propagation pathway was blocked. Unless the surface fire intensity reached a certain value, it was difficult to spread upwards to the canopy (Homainejad et al., 2022). In contrast, the threshold for fire spread in the canopy of P1 and P2 plantations was significantly higher than that of other stands because of the lower canopy weight of these two forest types, and because of the smallest forest age, the leaf moisture content was higher than that of other forest stands (Pook and Gill, 1993), which is required for higher fire intensity for leaf drying during canopy fire propagation (Balaguer-Romano et al., 2020). *C. equisetifolia* plantations in 20a (P3) had the highest probability of igniting canopy fires and smoldering canopy fires. Additionally, as an important factor in the model simulation, the crown fire is based largely on field observations and theoretical considerations (Cruz et al., 2005), therefore, special attention should be paid in the on-field observing on the crown fire to preventing them from smoldering canopy fires to avoid greater damage to the trees when managing forest fires in our study afterwards.

Conclusion

In this study, the load-weighted Rothermel model and the ignition observation test was adopted, which were mainly compared based on factors such as forest fire propagation speed, fire line intensity, and flame height, surface combustible material beds, and canopy fire behavior, which had a greater influence on the forest fire behavior characteristics of *C. equisetifolia* plantations. There have not been any studies on the interannual variation in the load of different types of combustibles. However, this study conducted a sample survey of only 69 subclasses of *C. equisetifolia* plantations for surface combustible loads and there is a lack of medium- and long-term investigations

http://www.aloki.hu ● ISSN 1589 1623 (Print) ● ISSN 1785 0037 (Online)
DOI: http://dx.doi.org/10.15666/aeer/2104_30753094

of the changes in the load of combustibles in forests. Therefore, in future studies, the change law of combustible material load on the surface can be determined according to the growth of different forest types, and then the change law of long-term potential forest fire behavior can be calculated. This provides a solid theoretical framework for forestry workers to employ in order to better prevent forest fires.

Acknowledgment. The study was financially supported by the Scientific and Technological Innovation Plan of Higher Education Institutions of Shanxi Province (2021L610); Hunan Provincial Natural Science Foundation of China (2022JJ40193).

REFERENCES

[1] Alteyrac, J., Cloutier, A., Zhang, S. Y. (2006): Characterization of juvenile wood to mature wood transition age in black spruce (Picea mariana (Mill.) BSP) at different stand densities and sampling heights. – Wood Science and Technology 40(2): 124-138.

[2] Andrews, P. L. (2018): The Rothermel surface fire spread model and associated developments: a comprehensive explanation. – Gen. Tech. Rep. RMRS-GTR-371. Fort Collins, CO: US Department of Agriculture, Forest Service, Rocky Mountain Research Station 371: 121.

[3] Andrews, P. L., Cruz, M. G., Rothermel, R. C. (2013): Examination of the wind speed limit function in the Rothermel surface fire spread model. – International Journal of Wildland Fire 22(7): 959-969.

[4] Ascoli, D., Russo, L., Giannino, F., Siettos, C., Moreira, F. (2018): Firebreak and Fuelbreak. – In: Manzello, S. L. (ed.) Encyclopedia of Wildfires and Wildland-Urban Interface (WUI) Fires. Springer, Cham, pp. 1-9.

[5] Bai, Y., Zhou, Y., Gong, J. (2021): Physiological mechanisms of the tolerance response to manganese stress exhibited by *Casuarina equisetifolia*, a candidate plant for the phytoremediation of Mn-contaminated soil. – Environmental Science and Pollution Research 28(33): 45422-45433.

[6] Balaguer-Romano, R., Díaz-Sierra, R., Madrigal, J., Voltas, J., Resco de Dios, V. (2020): Needle senescence affects fire behavior in Aleppo pine (Pinus halepensis Mill.) stands: a simulation study. – Forests 11(10): 1054.

[7] Bridges, J. M., Petropoulos, G. P., Clerici, N. (2019): Immediate changes in organic matter and plant available nutrients of Haplic Luvisol soils following different experimental burning intensities in Damak Forest, Hungary. – Forests 10(5): 453.

[8] Byram, G. M. (1959): Combustion of Forest Fuels. – In: Davis, K. P. Forest Fire: Control and Use. McGraw-Hill Book Company, New York, pp. 77-84.

[9] Crecente-Campo, F., Pommerening, A., Rodríguez-Soalleiro, R. (2009): Impacts of thinning on structure, growth and risk of crown fire in a *Pinus sylvestris L*. plantation in northern Spain. – Forest Ecology and Management 257(9): 1945-1954.

[10] Cruz, M. G., Alexander, M. E., Wakimoto, R. H. (2005): Development and testing of models for predicting crown fire rate of spread in conifer forest stands. – Canadian Journal of Forest Research 35(7): 1626-1639.

[11] Dai, E. F., Wang, X. L., Zhu, J. J., Xi, W. M. (2017): Quantifying ecosystem service trade-offs for plantation forest management to benefit provisioning and regulating services. – Ecology and Evolution 7(19): 7807-7821.

[12] Davies, G. M., Legg, C. J. (2011): Fuel moisture thresholds in the flammability of Calluna vulgaris. – Fire Technology 47(2): 421-436.

[13] Dymov, A. A., Startsev, V. V., Milanovsky, E. Y., Valdes-Korovkin, I. A., Farkhodov, Y. R., Yudina, A. V., ... Guggenberger, G. (2021): Soils and soil organic matter

http://www.aloki.hu ● ISSN 1589 1623 (Print) ● ISSN 1785 0037 (Online)
DOI: http://dx.doi.org/10.15666/aeer/2104_30753094

transformations during the two years after a low-intensity surface fire (Subpolar Ural, Russia). – Geoderma 404: 115278.
[14] García-Llamas, P., Suárez-Seoane, S., Taboada, A., Fernández-Manso, A., Quintano, C., Fernández-García, V., ... Calvo, L. (2019): Environmental drivers of fire severity in extreme fire events that affect Mediterranean pine forest ecosystems. – Forest Ecology and Management 433: 24-32.
[15] Geng, X., Cai, Z., Jia, S., Shen, J., Tang, D., Wang, D., Chen, S. (2022): Environmental Determinants of the Distribution of Halophila beccarii Ascherson in Hainan Island, China. – Sustainability 14(20): 13491.
[16] Gonçalves, A. C., Sousa, A. M. O. (2017): The Fire in the Mediterranean Region: A Case Study of Forest Fires in Portugal. – In: Fuerst-Bielis, B. (ed.) Mediterranean Identities - Environment, Society, Culture. IntechOpen, London, pp. 305-335.
[17] González-De, Vega. S., De las Heras, J., Moya, D. (2016): Resilience of Mediterranean terrestrial ecosystems and fire severity in semiarid areas: responses of Aleppo pine forests in the short, mid and long term. – Science of the Total Environment 573: 1171-1177.
[18] Holden, Z. A., Morgan, P., Evans, J. S. (2009): A predictive model of burn severity based on 20-year satellite-inferred burn severity data in a large southwestern US wilderness area. – Forest Ecology and Management 258(11): 2399-2406.
[19] Homainejad, N., Zlatanova, S., Pfeifer, N. (2022): A voxel-based method for the three-dimensional modelling of heathland from Lidar point clouds: first results. – ISPRS Annals of the Photogrammetry, Remote Sensing and Spatial Information Sciences 3: 697-704.
[20] Hu, H. Q., Liu, Y. C., Jiao, Y. (2007): Estimation of the carbon storage of forest vegetation and carbon emission from forest fires in Heilongjiang Province, China. – Journal of Forestry Research 18(1): 17-22.
[21] Huan-Ting, Z., Tie-Song, L., De-Yan, Z. (1994): Improvement of natural environments of coastal zone in South China. – Oceanology of China Seas 2: 497-506.
[22] Ji, C., Liu, H., Cha, Z., Lin, Q., Feng, G. (2022): Spatial-temporal variation of N, P, and K stoichiometry in cropland of Hainan Island. – Agriculture 12(1): 39.
[23] Khan, M. A., Khan, A. A., Usmani, A. S., Huang, X. (2022): Can fire cause the collapse of Plasco Building: a numerical investigation. – Fire and Materials 46(3): 560-575.
[24] Kreye, J. K., Varner, J. M., Hiers, J. K., Mola, J. (2013): Toward a mechanism for eastern North American forest mesophication: differential litter drying across 17 species. – Ecological Applications 23(8): 1976-1986.
[25] Kreye, J. K., Kane, J. M., Varner, J. M., Hiers, J. K. (2020): Radiant heating rapidly increases litter flammability through impacts on fuel moisture. – Fire -cology 16(1): 1-10.
[26] Kuznetsov, G. V., Nigay, N. A., Syrodoy, S. V., Gutareva, N. Y., Malyshev, D. Y. (2022): A comparative analysis of the characteristics of the water removal processes in preparation for incineration of typical wood waste and forest combustible materials. – Energy 239: 122362.
[27] Lands, G., Fernie, B. C. (2022): Recommendations for wildfire hazard reduction. – B.A. Blackwell & Associates Ltd, British Columbia.
[28] Li, X., Jin, H., Wang, H., Wu, X., Huang, Y., He, R., ... Jin, X. (2020a): Distributive features of soil carbon and nutrients in permafrost regions affected by forest fires in northern Da Xing'anling (Hinggan) Mountains, NE China. – Catena 185: 104304.
[29] Li, X. H., Sun, X. L., Dai, H. Y., Chen, S. H. (2020b): quantitative study on the grade of forest combustibles based on" 3S" technology. – Meteorological & Environmental Research 11(6).
[30] Li, X. Y., Jin, H. J., Wang, H. W., Marchenko, S. S., Shan, W., Luo, D. L., ... Jia, N. (2021): Influences of forest fires on the permafrost environment: a review. – Advances in Climate Change Research 12(1): 48-65.
[31] Malvar, M. C., Martins, M. A., Nunes, J. P., Robichaud, P. R., Keizer, J. J. (2013): Assessing the role of pre-fire ground preparation operations and soil water repellency in

http://www.aloki.hu ● ISSN 1589 1623 (Print) ● ISSN 1785 0037 (Online)
DOI: http://dx.doi.org/10.15666/aeer/2104_30753094

post-fire runoff and inter-rill erosion by repeated rainfall simulation experiments in Portuguese eucalypt plantations. – Catena 108: 69-83.

[32] Manzello, S. L., Suzuki, S., Gollner, M. J., Fernandez-Pello, A. C. (2020): Role of firebrand combustion in large outdoor fire spread. – Progress in Energy and Combustion Science 76: 100801.

[33] McAllister, S., Grenfell, I., Hadlow, A., Jolly, W. M., Finney, M., Cohen, J. (2012): Piloted ignition of live forest fuels. – Fire Safety Journal 51: 133-142.

[34] McCaw, W. L., Gould, J. S., Cheney, N. P., Ellis, P. F., Anderson, W. R. (2012): Changes in behaviour of fire in dry eucalypt forest as fuel increases with age. – Forest Ecology and Management 271: 170-181.

[35] Molina, A. J., del Campo, A. D. (2012): The effects of experimental thinning on throughfall and stemflow: a contribution towards hydrology-oriented silviculture in Aleppo pine plantations. – Forest Ecology and Management 269: 206-213.

[36] Molina, J. R., Ortega, M., y Silva, F. R. (2022): Fire ignition patterns to manage prescribed fire behavior: application to Mediterranean pine forests. – Journal of Environmental Management 302: 114052.

[37] Page, W., Jenkins, M. J. (2007): Predicted fire behavior in selected mountain pine beetle–infested lodgepole pine. – Forest Science 53(6): 662-674.

[38] Pausas, J. G., Paula, S. (2012): Fuel shapes the fire–climate relationship: evidence from Mediterranean ecosystems. – Global Ecology and Biogeography 21(11): 1074-1082.

[39] Petersson, L. K., Dey, D. C., Felton, A. M., Gardiner, E. S., Löf, M. (2020): Influence of canopy openness, ungulate exclosure, and low-intensity fire for improved oak regeneration in temperate Europe. – Ecology and Evolution 10(5): 2626-2637.

[40] Pook, E. W., Gill, A. M. (1993): Variation of live and dead fine fuel moisture in *Pinus radiata* plantations of the Australian-Capital-Territory. – International Journal of Wildland Fire 3(3): 155-168.

[41] Porterie, B., Morvan, D., Loraud, J. C., Larini, M. (2000): Firespread through fuel beds: modeling of wind-aided fires and induced hydrodynamics. – Physics of fluids 12(7): 1762-1782.

[42] Rajasekaran, T., Sruthi, J., Revathi, S., Raveena, N. (2015): Forest Fire Prediction and Alert System Using Big Data Technology. – In: Kunasekaran, K. K. H. et al. (eds.) Proceedings of the International Conference on Information Engineering, Management and Security, ICIEMS. Association of Scientists, Developers and Faculties, India, pp. 23-26.

[43] Roberts, G., Wooster, M. J., Lauret, N., Gastellu-Etchegorry, J. P., Lynham, T., McRae, D. (2018): Investigating the impact of overlying vegetation canopy structures on fire radiative power (FRP) retrieval through simulation and measurement. – Remote Sensing of Environment 217: 158-171.

[44] Rodrigues, C. A., Zirondi, H. L., Fidelis, A. (2021): Fire frequency affects fire behavior in open savannas of the Cerrado. – Forest Ecology and Management 482: 118850.

[45] Rothermel, R. C. (1972): A Mathematical Model for Predicting Fire Spread in Wildland Fuels. – Intermountain Forest & Range Experiment Station, Forest Service, US Department of Agriculture, Washington, DC.

[46] Rowell, E., Loudermilk, E. L., Seielstad, C., O'Brien, J. J. (2016): Using simulated 3D surface fuelbeds and terrestrial laser scan data to develop inputs to fire behavior models. – Canadian Journal of Remote Sensing 42(5): 443-459.

[47] Salem, M. Z., Mervat, E. H., Ali, H. M., Abdel-Megeed, A., El-Settawy, A. A., Böhm, M., ... Salem, A. Z. (2021): Plants-derived bioactives: novel utilization as antimicrobial, antioxidant and phytoreducing agents for the biosynthesis of metallic nanoparticles. – Microbial Pathogenesis 158: 105107.

[48] Splawinski, T. B., Cyr, D., Gauthier, S., Jetté, J. P., Bergeron, Y. (2019): Analyzing risk of regeneration failure in the managed boreal forest of northwestern Quebec. – Canadian Journal of Forest Research 49(6): 680-691.

http://www.aloki.hu ● ISSN 1589 1623 (Print) ● ISSN 1785 0037 (Online)
DOI: http://dx.doi.org/10.15666/aeer/2104_30753094

[49] Sullivan, A. L., McCaw, W. L., Cruz, M. G., Matthews, S., Ellis, P. F. (2012): Fuel, Fire Weather and Fire Behaviour in Australian Ecosystems. – In: Bradstock, R. A. et al. (eds.) Flammable Australia: Fire Regimes, Biodiversity and Ecosystems in a Changing World. CSIRO, Canberra, pp. 51-77.
[50] Taş, N., Prestat, E., McFarland, J. W., Wickland, K. P., Knight, R., Berhe, A. A., ... Jansson, J. K. (2014): Impact of fire on active layer and permafrost microbial communities and metagenomes in an upland Alaskan boreal forest. – The ISME Journal 8(9): 1904-1919.
[51] Valdivieso, J. P., Rivera, J. D. (2014): Effect of wind on smoldering combustion limits of moist pine needle beds. – Fire Technology 50(6): 1589-1605.
[52] Verma, S., Jayakumar, S. (2018): Effect of recurrent fires on soil nutrient dynamics in a tropical dry deciduous forest of Western Ghats, India. – Journal of Sustainable Forestry 37(7): 678-690.
[53] Wang, S., Huang, X., Chen, H., Liu, N. (2016): Interaction between flaming and smouldering in hot-particle ignition of forest fuels and effects of moisture and wind. – International Journal of Wildland Fire 26(1): 71-81.
[54] Wu, Z., He, H. S., Keane, R. E., Zhu, Z., Wang, Y., Shan, Y. (2019): Current and future patterns of forest fire occurrence in China. – International Journal of Wildland Fire 29(2): 104-119.
[55] Wu, Z., Li, M., Wang, B., Tian, Y., Quan, Y., Liu, J. (2022): Analysis of factors related to forest fires in different forest ecosystems in China. – Forests 13(7): 1021.
[56] Zhang, Y. H., Sun, M. L., Liu, T. (2012): Effect of forest fire on soil physical and chemical properties of typical forests in Daxing'an Mountains. – Journal of Northeast Forestry University 40(6): 41-107.
[57] Zhang, Z., Long, T., He, G., Wei, M., Tang, C., Wang, W., ... Zhang, X. (2020): Study on global burned forest areas based on Landsat data. – Photogrammetric Engineering & Remote Sensing 86(8): 503-508.
[58] Zhou, X., Sun, H., Pumpanen, J., Sietiö, O. M., Heinonsalo, J., Köster, K., Berninger, F. (2019): The impact of wildfire on microbial C:N:P stoichiometry and the fungal-to-bacterial ratio in permafrost soil. – Biogeochemistry 142: 1-17.
[59] Zhu, H., Gao, D., Zhang, S. (2019): A perceptron algorithm for forest fire prediction based on wireless sensor networks. – Journal on Internet of Things 1(1): 25.

http://www.aloki.hu ● ISSN 1589 1623 (Print) ● ISSN 1785 0037 (Online)
DOI: http://dx.doi.org/10.15666/aeer/2104_30753094